

Photodynamic therapy of multidrug resistant leukemic murine cells by 3,6-bis(alkylthiourea)acridine hydrochlorides

Helena PAULÍKOVÁ^{1*}, Alžbeta CISÁRIKOVÁ¹, Zuzana BAČOVÁ², Ladislav JANOVEC³, Ján IMRICH³, Mário ŠEREŠ⁴, Luba HUNÁKOVÁ⁵

¹Department of Biochemistry and Microbiology, Slovak University of Technology, Bratislava, Slovakia; ²Institute of Experimental Endocrinology, Biomedical Research Center, Slovak Academy of Sciences, Bratislava, Slovakia; ³Department of Organic Chemistry, Pavol Jozef Šafárik University, Košice, Slovakia; ⁴Institute of Molecular Physiology and Genetics, Slovak Academy of Sciences, Bratislava, Slovakia; ⁵Institute of Immunology, Faculty of Medicine, Comenius University in Bratislava, Bratislava, Slovakia

*Correspondence: helena.paulikova@stuba.sk; paulikhe@gmail.com

Received March 24, 2021 / Accepted June 10, 2021

Efforts to overcome multidrug resistance in cancer have led to the development of several novel strategies including photodynamic therapy (PDT). PDT is based on the use of photosensitizers (PSs) photoactivation, which causes the formation of reactive oxygen species that can induce cell death. In the last decade, the development of new PSs has been significantly accelerated. Recently, acridine-3,6-dialkyldithiourea hydrochlorides (AcrDTUs) have been investigated as a new group of PSs and we have shown that PDT/AcrDTUs caused cell death of mouse leukemic cells L1210. In this study, we investigated the efficacy of PDT/AcrDTUs for the treatment of L1210/VCR cells as a model of chemoresistant cells (overexpressing P-glycoprotein, P-gp). The photoactivation (365 nm, 1.05 J/cm²) increased the cytotoxicity of AcrDTUs 10–15 times. Inhibition of P-gp (verapamil) has been shown to have no significant effect on the accumulation of propyl-AcrDTU (the most potent derivative) in L1210/VCR cells. The intracellular distribution of this acridine derivative has been studied. Prior to irradiation of the resistant cells, propyl-AcrDTU was sequestered mainly in the cytosol, partly in the mitochondria, and, unlike in the sensitive cells, the AcrDTU was not found in the lysosomes. PDT with 1 μM propyl-AcrDTU induced cell shrinkage and “ladder DNA” formation, and although a drastic decrease of the intracellular ATP level was observed at the same time, there was no increase in extracellular LDH activity. AIF in the nucleus can induce DNA fragmentation and we have actually observed a mitochondrio-nuclear translocation of AIF. We concluded that AcrDTUs are photocytotoxic against L1210/VCR cells and that mitochondria play an important role in cell death induced by PDT.

Key words: photodynamic therapy, photosensitizers, acridine, multidrug resistance, leukemia cells

The major complication of cancer chemotherapy is the development of multidrug resistance (MDR). MDR is a phenomenon that involves a number of factors, including the overexpression of drug efflux transporters [1–5]. Efforts to overcome multidrug resistance in cancer have led to the development of several new strategies and results obtained by several research teams have shown the possibility of treating MDR tumors with photodynamic therapy (PDT) [6–9]. PDT involves the administration of a photosensitizer (PS), followed by irradiation of the tumor with visible or UV-A light. The main group of photosensitizers (PSs) used today in clinical PDT are porphyrins, yet the number of non-porphyrin PDT candidates continues to increase. A group of non-porphyrin PSs is acridine derivatives. Although UV-A light is not preferred in conventional PDT, the emission property of acridines has been used for cellular imaging to study their localization inside the cells [10]. MDR

involves a number of factors, and this phenomenon is most commonly associated with the uptake of drugs. Overproduction of the ABC transporters can export drugs from cells or accumulate them in vesicles. In particular, overproduction of P-glycoprotein (P-gp), multidrug resistance-associated protein 1 (MRP1), and BCRP (breast cancer resistance protein)/ABCG2 transporter are related to MDR [11–14]. The photocytotoxicity of many PSs against MDR cells was evaluated. Some of them (e.g., methylene blue, pheophorbide a, acridine orange (AO), and some of the porphyrin derivatives) were effective in removing P-gp-expressing tumor cells and even act as reversers of MDR [7–10, 15–18].

Some of the selective and potent anticancer acridine derivatives synthesized in the last decades [19–23] also exhibited photosensitizing properties [24–28]. For example, photocytotoxicity of AO [29, 30] allowed the *in vivo* treatment of musculoskeletal sarcoma [31–35]. Recently, antitumor

activities and photocytotoxicity of novel acridine derivatives, 3,6-bis(alkylthiourea)acridine hydrochlorides (AcrDTUs), have been studied [36]. The superoxide radical anion formed after irradiation of AcrDTU with UV-A light above 300 nm has been confirmed by an EPR study and we confirmed that AcrDTUs are photocytotoxic against L1210 mouse leukemia cells. Photocytotoxicity of propyl-AcrDTU against the NIH-3T3 line was approximately 8-times lower than against the leukemia cells L1210 [36]. The IC_{50} of the most photocytotoxic propyl-AcrDTU was $0.48 \pm 0.03 \mu\text{M}$. After irradiation (365 nm, 1.05 J/cm^2), ROS production led to lysosomal photodestruction and spillage of lysosomal enzymes into the cytoplasm, resulting in cellular death. L1210/S cells can be turned into a multidrug resistant L1210/VCR cell line that expresses P-glycoprotein (P-gp) by stepwise adaptation to vincristine (VCR) [37–39]. In this study, the multidrug resistant L1210/VCR subline of mouse leukemic cells was used as a model for studying the *in vitro* efficacy of acridine derivatives against MDR cells. The cytotoxic effects of AcrDTUs against drug resistant L1210/VCR mouse leukemic cells were evaluated without irradiation and after irradiation with UV-A light at 365 nm. The mechanism of photocytotoxicity of propyl-AcrDTU as the most potent derivative was investigated. ROS generation in irradiated L1210/VCR was monitored without and after AcrDTU treatment. Cellular uptake of propyl-AcrDTU and the effect of P-gp transport activity on propyl-AcrDTU photocytotoxicity were evaluated. Finally, our attention was focused on the intracellular localization of propyl-AcrDTU in order to explain the mechanism of the photocytotoxic effect of these PSs against resistant cells.

Materials and methods

Materials. Dimethyl sulfoxide (DMSO), Triton X-100, propidium iodide (PI), (dimethylthiazol-2-yl)-2,5-diphenyltetrazolium bromide (MTT), RPMI-1640 medium, agarose, MitoRed, dihydroethidium (DHE), penicillin, streptomycin, fetal bovine serum (FBS), phosphate buffered saline (PBS), Trolox, 2-amino-2-hydroxymethyl-1,3-propanediol (TRIS), ethylenedinitrilotetraacetic acid (EDTA), proteinase K, RNase A, ATP bioluminescence assay kit, β -nicotinamide adenine dinucleotide (NADH), Hoechst 33342, glycerol, verapamil, bromophenol blue, Tri Reagent, primary antibody anti-rabbit AIF, and secondary antibody anti-rabbit IgG Texas Red[®] were all obtained from Sigma-Aldrich (Germany). A Tetro cDNA Synthesis Kit and a SensiFAST[™] SYBR[®]-No-ROX Kit were obtained from Bioline (USA). Nuclease-free water was from MP Biomedicals (USA). A FlowCelect Annexin Red Kit was bought from Merck-Millipore, a SytoRed, LysoTracker Deep Red from Life Technologies[™], GelRED from Biotium (USA), vincristine from Gedeon Richter Plc., and sodium chloride, methanol, ethanol, chloroform, isopropanol, pyruvate, and hydrochloric acid from Lachema (Czech Republic). Primers

(GAPDH, cathepsin B, and cathepsin D) were obtained from Ecoli (Slovakia). The studied 3,6-bis(alkylthiourea)acridine hydrochlorides (AcrDTUs) were prepared in our laboratory [40].

Cell culture conditions. The L1210/S mouse leukemia cell line and L1210/VCR resistance subline were grown in RPMI-1640 medium. The medium was supplemented with 10% FBS, penicillin (100 U/ml), and streptomycin (100 $\mu\text{g/ml}$). The cells were maintained at 37°C in a humidified 5% CO_2 atmosphere. The L1210/S and L1210/VCR cells were obtained from Dr. Z. Sulová, Institute of Molecular Physiology and Genetics, Slovak Academy of Sciences, Bratislava.

Irradiation of the cells. In all experiments, cells were irradiated with UV-A light (Philips UV lamp, 15 W) after 1 h incubation with AcrDTUs with a light dose of 1.05 J/cm^2 . Cells were irradiated directly in Petri dishes or culture plates. The same dose of light was used for all cell lines studied.

MTT assay. Cell viability (metabolic activity status) was determined using the MTT microculture tetrazolium assay as previously described [41]. Cells ($2 \times 10^5/\text{ml}$) were incubated with AcrDTUs (0–20 μM) in a 96-well culture plate in medium and irradiated after 1 h incubation (UV-A, 365 nm, 1.05 J/cm^2) or stored in the dark. Then the incubation was continued in the dark for 48 h and finally cell viability was determined.

Cytotoxic effect of verapamil. Cells ($2 \times 10^5/\text{ml}$) were preincubated with verapamil (1 μM) for 1 h. Propyl-AcrDTU (0–1.5 μM) was then added and after 1 h incubation, the cells were irradiated or stored in the dark. Viability after 48 h was determined by the MTT assay.

Intracellular accumulation of propyl-AcrDTU. Cells ($0.5 \times 10^6/\text{ml}$) were incubated with propyl-AcrDTU (1 μM) for 15 min, 1 h, and 6 h. After incubation with AcrDTU, cells were washed with PBS and visualized with a fluorescence microscope (Carl Zeiss, Axio ANO Imager A1, Germany).

ROS detection. ROS production in irradiated cells was determined by dihydroethidium (DHE). Cells ($1 \times 10^6/\text{ml}$) were incubated for 24 h at 37°C in Petri dishes in the medium. Propyl-AcrDTU (1 μM) and Trolox (100 μM) were then added. After 1 h, Petri dishes were stored in the dark or exposed to UV-A light (365 nm, 1.05 J/cm^2). After irradiation, DHE (20 μM) was added to each Petri dish and incubated at 37°C for 20 min. Subsequently, cells were washed with PBS, and fluorescence was observed with the Carl Zeiss Axio ANO Imager A1 fluorescence microscope (Germany).

Detection of nuclear DNA fragmentation. Cells ($1 \times 10^6/\text{ml}$) were incubated without (control) or with propyl-AcrDTU (1 μM) and irradiated. After 2, 4, and 6 h, cells were washed with PBS and centrifuged ($100 \times g$, 4 min). A lytic solution (10 mM Tris, pH 8, 1 mM EDTA, 0.5% Triton-X) was added to the pellet and the samples were frozen for 3 min at -20°C . Cellular lysates were incubated with proteinase K (1 mg/ml) for 30 min at 50°C . After heating at 70°C for

Table 1. Primer sequences.

Gene	Forward primer	Reverse primer
GAPDH	GTGTCCGTCGTGGATCTGAC	GGAGACAACCTGGTCCTCAG
Cathepsin B	CTTCCCATGTCGGCAATCAGAAC	AAGACATCTAGAGTACCCCAAG
Cathepsin D	CACGTCCTTTGACATCCACTACG	CAGCTCCTCACCTCTCCACAG

10 min, RNase (300 µg/ml) was added at 50 °C for 10 min. NaCl/EDTA solution (1 M NaCl, 2 mM EDTA) and isopropanol were then added for precipitation and stored at -20 °C for 12 h. After centrifugation (14,100× g, 20 min), the pellet was washed with 70% ethanol and dissolved in TE buffer (Tris-EDTA). The DNA was analyzed by electrophoresis on 1% agarose gel stained with GelRED (2 µl/50 ml). The gel was visualized with a UV transilluminator using a Kodak EasyShare Z612 camera.

LDH assay. The lactate dehydrogenase (LDH) assay was performed according to the method of Grivell and Berry [42]. Cells were treated with propyl-AcrDTU (0–2 µM) for 1 h and then irradiated (365 nm, 1.05 J/cm²). After 6 or 24 h of incubation, the cell medium (100 µl) was transferred to a cuvette containing 0.9 ml of the reaction mixture to give a final concentration of 1 mM pyruvate, 0.15 mM NADH, and 104 mM phosphate buffer (pH 7.4). Maximum LDH release was determined by the lysis of cells. Absorbance at 366 nm was recorded using an Analytic Jena Specord 250 spectrophotometer.

Determination of ATP levels. The level of intracellular ATP was determined using a bioluminescence kit measuring the light output from the luciferin-luciferase reaction. Cells (1×10⁶/ml) were treated with propyl-AcrDTU (1 µM) and irradiated. After 2, 4, and 6 h, the cells were washed and ATP content was measured in quadruplicate (1×10⁵ cells/100 µl) according to the manufacturer's protocol. Results were expressed as a percentage of the control.

Co-localization of AcrDIM with cell organelles. L1210/VCR cells (0.5×10⁶) were treated with 2 µM propyl-AcrDTU (37 °C) for 1 h and then irradiated or stored in the dark. After incubation with AcrDTU, samples were labeled with SytoRed (0.1 µM, 35 min) to visualize cell nuclei, or MitoRed (0.1 µM, 15 min) to label mitochondria or LysoTracker Deep Red (0.1 µM, 25 min) to label lysosomes. After incubation with the fluorescence dyes, cells were washed twice with PBS and immediately visualized with an Amnis ImageStream Imaging Flow Cytometer: VIS (channel 1), AcrDTU (channel 2), MitoRed (channel 3), LysoTracker (channel 11), SytoRed (channel 11). The Bright Detail Similarity Functions were calculated for a double-positive, single, and focused cell population.

Analysis of AIF translocation to nuclei. Cells (2×10⁵/ml) were treated with 1 µM propyl-AcrDTU for 1 h and exposed to UV-A light (365 nm, 1.05 J/cm²). After 2 and 4 h incubation, cells were washed with PBS and embedded on poly-L-lysine coated microscope slides. The cells were then washed and fixed with methanol (4 °C, 20 min). After 24 h of incubation

with anti-AIF antibody, cells were labeled with the secondary antibody (IgG Texas Red[®]) for 2 h at 4 °C. Cell nuclei were labeled with Hoechst 33342 and monitored using a Zeiss Axiovert 200M confocal microscope (63×/1.4 oil objective).

Cathepsins expression – RT-PCR. Total RNA was extracted and purified from a homogenate of L1210/S and L1210/VCR cells (2×10⁶). Cells were lysed in Tri Reagent (300 µl), nuclease-free water (300 µl), and chloroform (100 µl) for 3 min. The samples were centrifuged (14,100×g, 15 min, 4 °C) and the aqueous phase containing RNA was then incubated with isopropanol for 10 min. After further centrifugation (14,100×g, 10 min), the pellet was washed with 75% ethanol and stored at -20 °C. The amount, integrity, and purity of the RNA were determined with a NanoDrop2000 spectrophotometer. RNA was reverse transcribed to cDNA using a Tetro cDNA Synthesis Kit according to the manufacturer's protocol in 20 µl volume by incubation at 45 °C for 30 min and 85 °C for 5 min, followed by maintenance at 4 °C. The first-strand cDNA was stored at -20 °C until use. Quantitative RT-PCR was performed on AB7900 using a SensiFAST™ SYBR® No-ROX Kit. The reaction solution contained a master mix (20 µl), 0.3 µmol/l for each forward and reverse primer (Table 1), a 2 µM ROX reference dye, and a cDNA template (10 ng). PCR was performed for 50 cycles according to the following protocol: activation of Taq polymerase at 95 °C for 15 min, followed by 50 cycles of denaturation at 95 °C for 15 s, annealing at 60 °C for 1 min, and extension at 72 °C for 1 min, followed by fluorescence measurement (SYBR Green and ROX, respectively). A melting curve analysis was performed to identify the reaction products. Relative mRNA expression was calculated by the Livak method [43] for analysis of relative gene expression with a comparative threshold of 2^{-ΔΔC_t}. The data from gene expression analysis are reported as the ratio of the target gene in L1210/VCR cells to that in L1210/S cells and normalized to express the reference gene, GAPDH. The baseline expression level of L1210/S cells was set to 1.

Statistical analysis. Data are expressed as a mean ± standard error (SD). Statistical data analyzes were performed using standard one-way ANOVA procedures. The differences between the mean values were considered significant when p-values were <0.05.

Results

Cytotoxicity and photocytotoxicity. Photocytotoxicity of AcrDTUs against L1210/VCR and L1210/S mouse leukemia

cells was evaluated by MTT assay. Since irradiation of cells without AcrDTUs with UV-A light (1.05 J/cm^2) for 5 min had no effect on cell viability, this dose was used in all subsequent experiments. The irradiation increased the cytotoxicity of all AcrDTU derivatives against resistant cells about 10 times acromolecules leads to damages of the subcellular structures. The superoxide radical is formed after irradiation of AcrDTU [36] and DHE can be used as a probe of the formation of ROS in the treated cells. As shown in Figure 1A, PDT/propyl-AcrDTU induced oxidative stress in L1210/VCR cells and the addition of Trolox, a soluble form of vitamin E, reduced superoxide radical levels (Figure 1A) and consequently the photocytotoxicity of propyl-AcrDTU decreased (Figure 1B), but only by 11%. Thus, Trolox could not completely eliminate the ROS photoproduction.

Intranucleosomal fragmentation. Oxidative cytotoxicity includes apoptosis and autophagy as well as cellular necrosis. PDT-mediated oxidative stress is negatively modulated by intracellular antioxidant defense by superoxide dismutase, catalase, or glutathione. L1210/VCR resistance is not associated with the overproduction of glutathione or antioxidant enzymes [44], and PDT-mediated oxidative stress can cause cell cycle arrest and cell death [45–48]. We found that the irradiation dose (1.05 J/cm^2) had no effect on the viability of L1210/VCR and analysis of intranucleosomal DNA fragmentation after PDT/propyl-AcrDTU confirmed the formation of a DNA ladder 6 h after the irradiation of L1210/VCR cells (Figure 2A).

Extracellular LDH and intracellular ATP levels. PDT induces several types of cell death (depending on PS and cancer cell lines) including apoptosis and necrosis, and previous evidence suggests the potential for these forms of cell death to coexist. Necrosis is characterized by a loss of plasma membrane integrity and, as shown in Figure 2B, the induction of necrosis was also confirmed by the observed release of the intracellular lactate dehydrogenase (LDH) enzyme. PDT with $1 \mu\text{M}$ propyl-AcrDTU increased the LDH activity

in the medium by approximately 17% 24 h after irradiation and at a higher concentration, $2 \mu\text{M}$ propyl-AcrDTU, LDH activity in the medium increased by about 32% compared to control (Figure 2B). In addition, PDT with $1 \mu\text{M}$ propyl-AcrDTU reduced the ATP level by about 60% (Figure 2C). Since a substantial decrease in ATP levels is a typical sign of necrosis, propyl-AcrDTU after irradiation of the cells may hypothetically damage OXPHOS (oxidative phosphorylation system) in mitochondria. Since intracellular ATP levels may modulate externalization of phosphatidylserine during apoptosis, we supposed that drastic reduction in intracellular ATP levels after PDT (Figure 2C) could encourage necrotic rather than apoptotic cell death or apoptosis without typical symptoms occurred.

Accumulation of propyl-AcrDTU in L1210/VCR cells. Since AcrDTUs are fluorescent compounds [40], the intracellular uptake of propyl-AcrDTU, which can be rapid due to its hydrophobicity [40], was monitored by fluorescence microscopy. L1210/VCR cells were incubated with propyl-AcrDTU for 6 h and as shown in representative microphotographs (Figure 3A), the fluorescence signal was strong

Table 2. Cytotoxicity and photocytotoxicity of AcrDTUs against resistant L1210/VCR and sensitive L1210/S cells.

	IC ₅₀ (μM) 48 h			
	L1210/VCR		L1210/S*	
	Dark	UV-A	Dark	UV-A
Propyl-AcrDTU	9.15±1.54	1.32±0.21	5.70±1.03	0.48±0.03
Butyl-AcrDTU	13.30±2.04	1.58±0.40	6.60±0.93	0.52±0.09
Pentyl-AcrDTU	16.50±2.11	1.65±0.12	9.20±1.31	0.60±0.05

Notes: AcrDTU stock solutions were dissolved in DMSO and an equal volume of DMSO was added to control cells (final DMSO concentration was <0.2%). Cells were irradiated (1.05 J/cm^2) after 1 h incubation with AcrDTUs in the dark and viability was determined 48 h after addition of AcrDTUs by MTT assay. IC₅₀ values (μM) are concentrations that produce 50% inhibition of cell viability. Results are expressed as a mean ± SD (n=3). * - Published in [36].

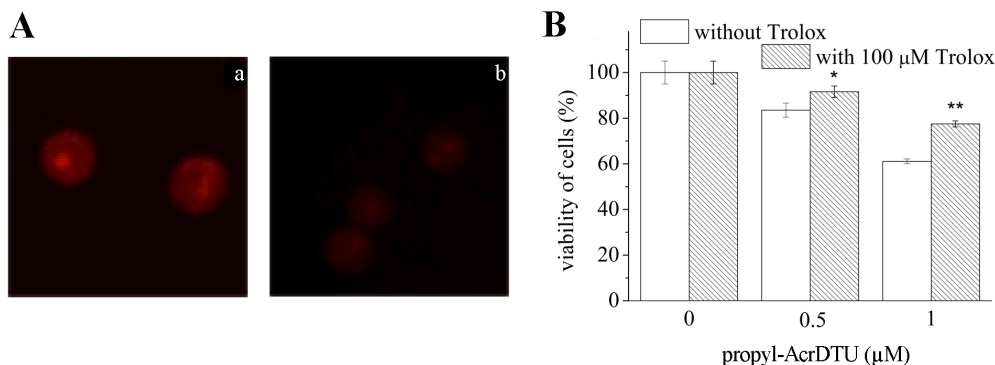


Figure 1. Oxidative stress induced by propyl-AcrDTU in L1210/VCR cells after cell irradiation. Oxidative stress was monitored by DHE staining immediately after cell irradiation (365 nm , 1.05 J/cm^2) A) Cells were treated with PDT/propyl-AcrDTU ($1 \mu\text{M}$) without (a) or with $100 \mu\text{M}$ Trolox (b). Microphotographs of the cells were obtained using the Carl Zeiss ANO Imager A1 fluorescence microscope (excitation 535 nm ; emission 620 nm). Magnification: $40\times$. Cell viability in the presence of Trolox (B) was determined using the MTT assay 24 h after the addition of propyl-AcrDTU. Significant differences between the cells treated without and with Trolox were indicated as * $p < 0.005$, ** $p < 0.0001$.

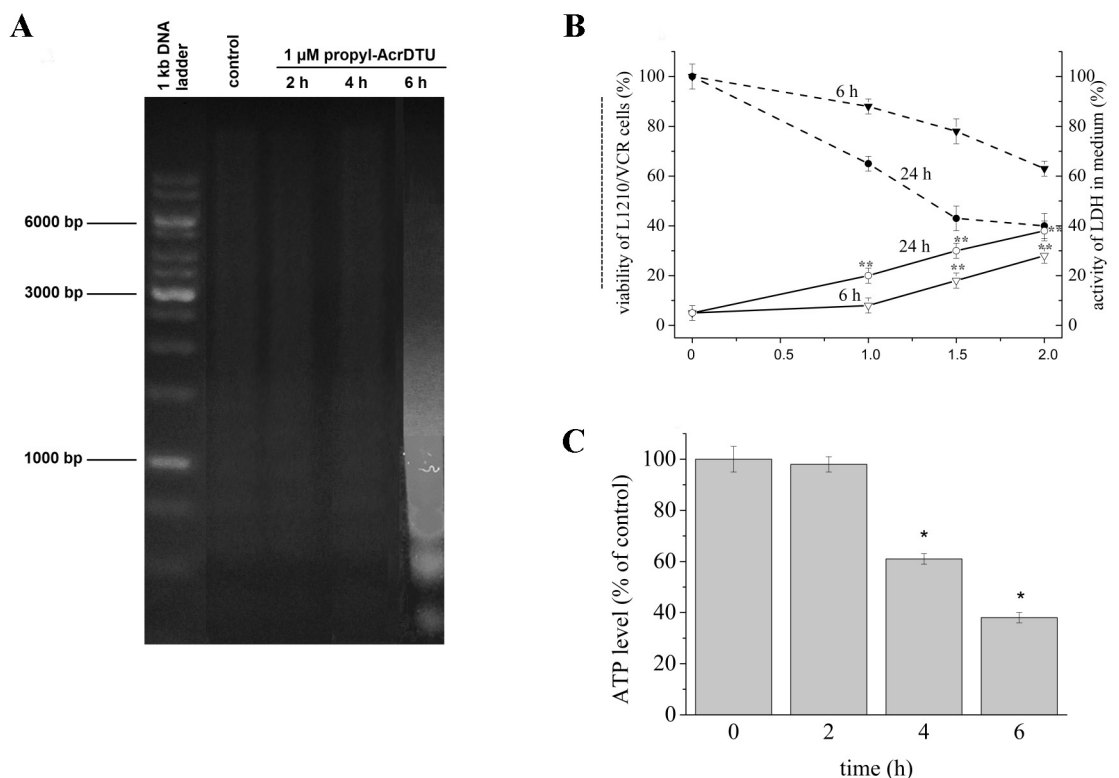


Figure 2. Analysis of cellular death induced by propyl-AcrDTU in L1210/VCR cells after cell irradiation. Detection of intranucleosomal fragmentation. A) L1210/VCR cells were treated with 1 μ M propyl-AcrDTU for 1 h and exposed to UV-A light (365 nm, 1.05 J/cm²). DNA fragmentation was visualized in a 1% agarose gel 6 h after the addition of propyl-AcrDTU. Control: irradiated cells without propyl-AcrDTU. LDH activity in medium and viability of L1210/VCR cells. B) Cells were treated with propyl-AcrDTU (1–2 μ M) for 1 h and then irradiated (365 nm, 1.05 J/cm²). LDH activity and cell viability (MTT assay) were determined after 6 h and 24 h of incubation. ATP levels in L1210/VCR cells. Significant differences between LDH activity in the medium of control cells and treated cells were indicated as ** $p < 0.001$. C) Cells were treated with 1 μ M propyl-AcrDTU for 1 h and exposed to UV-A light (365 nm, 1.05 J/cm²). Changes in ATP levels were assessed after 2, 4, and 6 h after the addition of propyl-AcrDTU. Results are expressed as a percent of control (mean \pm SD). Significant differences between irradiated control cells and treated cells were indicated as * $p < 0.005$.

even after 1 h of cell incubation and did not change after its prolongation. Overexpression of P-gp, which can effectively remove vincristine from cells, has been confirmed in L1210/VCR [37]. Drug exports may be inhibited by verapamil, a well-known inhibitor of P-gp activity [49]. To verify whether the intracellular accumulation of propyl-AcrDTU depends on P-gp activity, L1210/VCR cells were incubated with verapamil. As shown in Figure 3B, brightly shining AcrDTU microgranules were formed in the cytoplasm of resistant cells and the intensity of the propyl-AcrDTU fluorescence signal did not change significantly in the presence of verapamil (Figures 3Ba, 3Bb). Probably, as in resistant cells, verapamil had no effect on the number of fluorescent microgranules in sensitive L1210 cells (Figures 3Bc, 3Bd).

Verapamil is a potent inhibitor of P-gp and can almost completely reverse the drug resistance of L1210/VCR to vincristine [49]. However, we found that this P-gp inhibitor had a weak effect on propyl-AcrDTU photocytotoxicity and increased the photocytotoxicity of 1.5 μ M propyl-AcrDTU by only about 10% (Figure 3C).

Mechanism of photocytotoxicity and intracellular distribution of propyl-AcrDTU. PS can be localized in different organs, and it is this subcellular sequestration of PS that designates many signaling pathways that occur after PDT. To explain the mechanism of propyl-AcrDTU photocytotoxicity, its intracellular distribution was examined using the Amnis ImageStream Imaging Flow Cytometer using a green fluorescence derivative. Co-localizations of propyl-AcrDTU with the mitochondrial dye MitoRed, the lysosomal dye LysoTracker, and SytoRed nucleic acid stain were monitored. A Bright Detail Similarity R3 Feature reflects co-localization of two probes; no co-localization is characterized by values around 1, and perfect co-localization is represented by values close to 3.

First, co-localization of propyl-AcrDTU with the MitoRed mitochondrial probe was monitored and Bright Detail Similarity R3 Feature was calculated. The fluorescence of propyl-AcrDTU and MitoRed overlapped in resistant cells already before irradiation and their partial co-localization was demonstrated (Figure 4) by the Bright Similarity R3

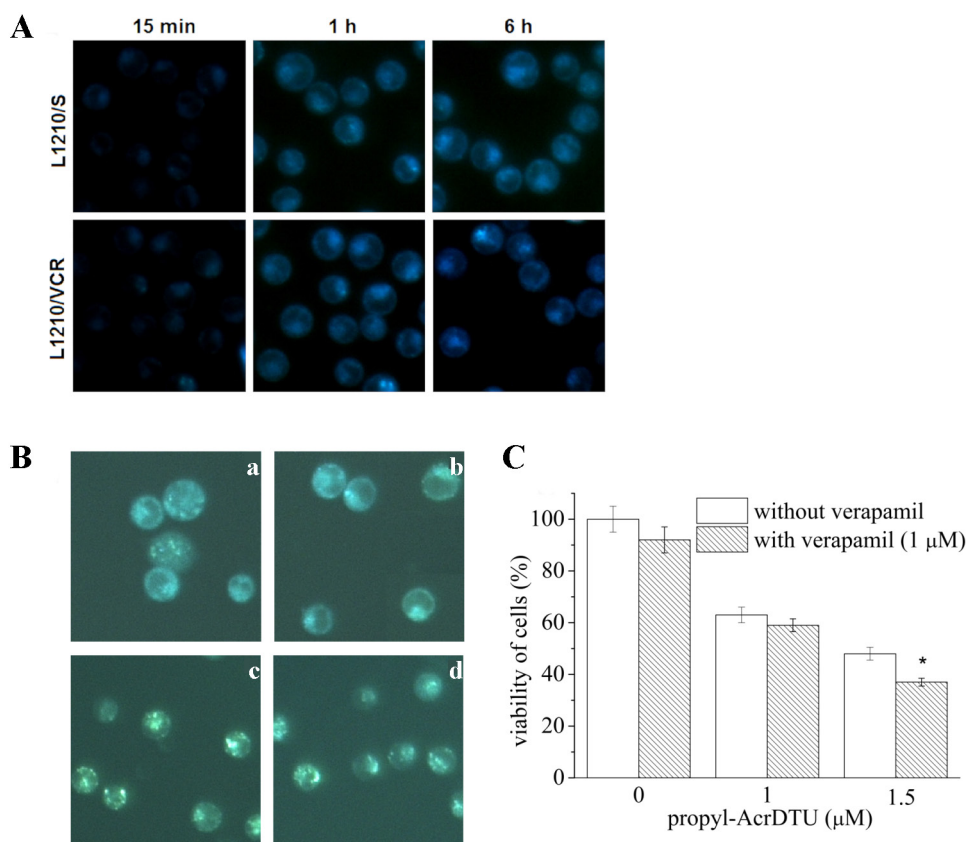


Figure 3. Accumulation of propyl-AcrDTU in the cells and the effect of verapamil on photocytotoxicity of propyl-AcrDTU. Uptake of propyl-AcrDTU into sensitive L1210/S and resistant L1210/VCR cells. **A)** Cells were incubated with 1 μM propyl-AcrDTU for 15 min, 1 h, and 6 h. Microphotographs of the cells were obtained using the Carl Zeiss ANO Imager A1 fluorescence microscope. Magnification: 40x10. Propyl-AcrDTU accumulation in the sensitive and resistant cells in the absence and presence of verapamil. **B)** L1210/VCR and L1210/S cells were preincubated with 1 μM verapamil for 1 h and then 2 μM propyl-AcrDTU was added. The accumulation of propyl-AcrDTU in the cells was analyzed after 48 h with the Carl Zeiss ANO Imager A1 fluorescence microscope. Magnification: 40x10. Photocytotoxicity of propyl-AcrDTU against the L1210/VCR cells in the presence of verapamil. **C)** Cells were treated with 1 μM verapamil for 1 h, then propyl-AcrDTU (1 and 1.5 μM) was added and after 1 h the cells were irradiated (365 nm, 1.05 J/cm²). Cell viability was determined after 48 h by MTT assay. Significant differences between treated cells without and with verapamil were indicated as **p*<0.05.

Feature in the range 1–1.5. Analysis of co-localization of propyl-AcrDTU and MitoRed in the irradiated cells showed that nearly 61% of the focused L1210/VCR cells were positive for both fluorescence dyes (the Bright Similarity R3 Feature was about 2.5).

The localization of propyl-AcrDTU in the L1210/VCR cell mitochondria (Figure 4) and a significant reduction in ATP levels after irradiation (Figure 2D) showed that mitochondrial membranes and/or OXPHOS complexes could be damaged by ROS. Together with the transfer of propyl-AcrDTU to the mitochondria, the release of pro-apoptotic mitochondrial proteins could occur. However, no activation of caspase-9 and caspase-3 was confirmed (results not shown), but relocalization of AIF into the nucleus was recorded (Figure 5).

Based on our previous results, we expected that propyl-AcrDTU would be trapped in acidic vesicles – lysosomes

in the protonated form, similar to L1210 sensitive cells [36]. Surprisingly, the propyl-AcrDTU fluorescence did not overlap with the LysoTracker fluorescence probe in L1210/VCR, where the Bright Similarity R3 Feature was about 1 (Figure 4). After irradiation of resistant cells, the relocation of propyl-AcrDTU to lysosomes was recorded (Bright Similarity R3 Feature was about 2.0; Figure 4).

In contrast to the sensitive cell line, sequestration of propyl-AcrDTU in lysosomes of the resistant L1210/VCR cells was not confirmed. For this reason, differences in lysosome biogenesis were expected between resistant L1210/VCR cells and sensitive L1210/S cells. Therefore, cathepsin B and D expression in resistant cells was compared to that in sensitive cells. RT-PCR analysis of cathepsin B and D expression in L1210/VCR and L1210/S cells showed that the cathepsin levels in resistant cells were several times lower than in parental L1210/S cells (Table 3). Noteworthy, propyl-

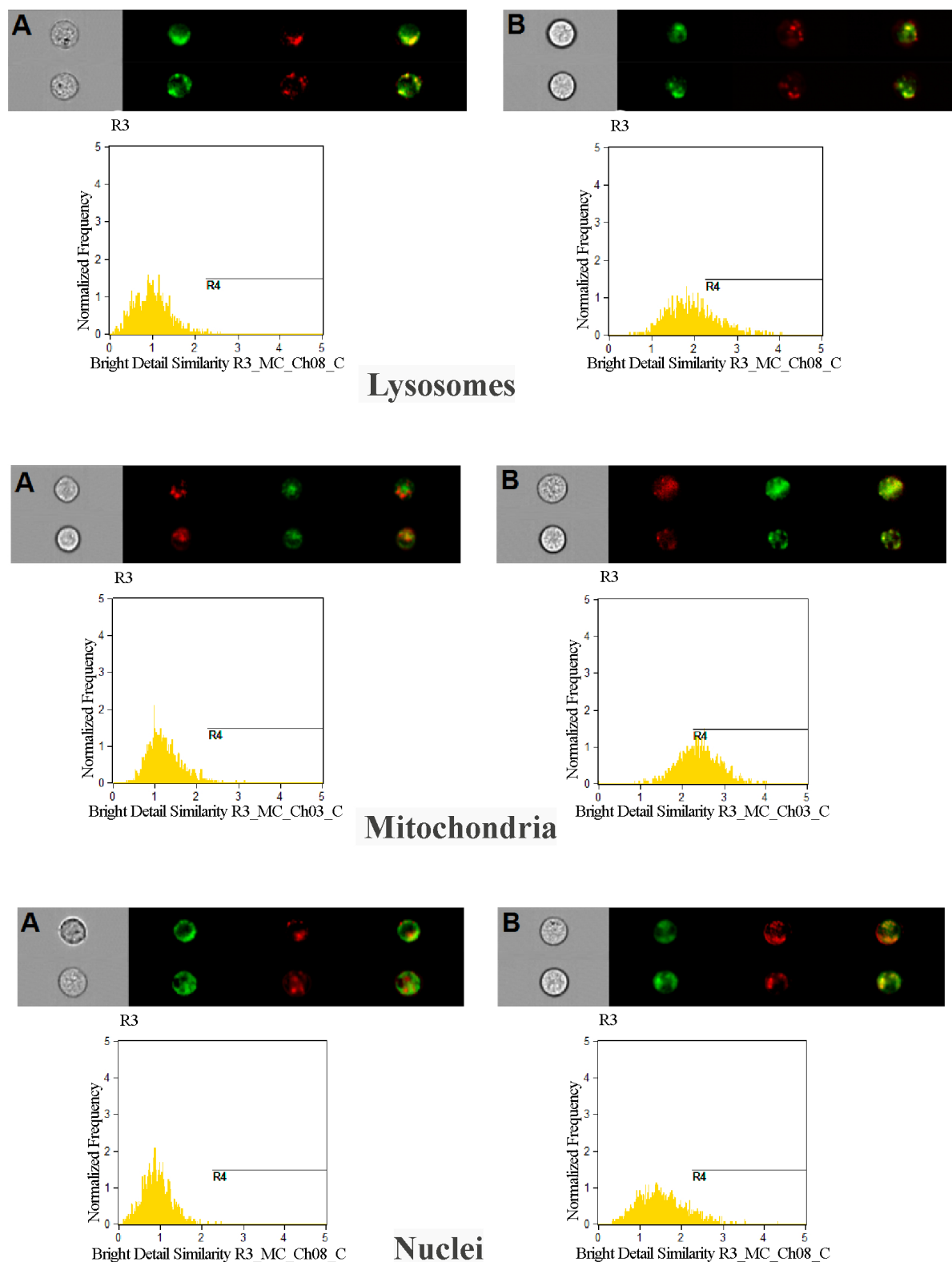


Figure 4. Localization of propyl-AcrDTU in L1210/VCR without (A) or with irradiation (B). Cells were treated with 2 μ M propyl-AcrDTU (green) for 1 h and exposed to UV-A light (365 nm, 1.05 J/cm²), mitochondria were labeled with the MitoRed (red), the lysosomes were labeled with the LysoTracker (red), and the nuclei were labeled with the SytoRed (red). Corresponding Bright Similarity R3 Features are shown below the photomicrographs. The R4 marker represents colocalized cells.

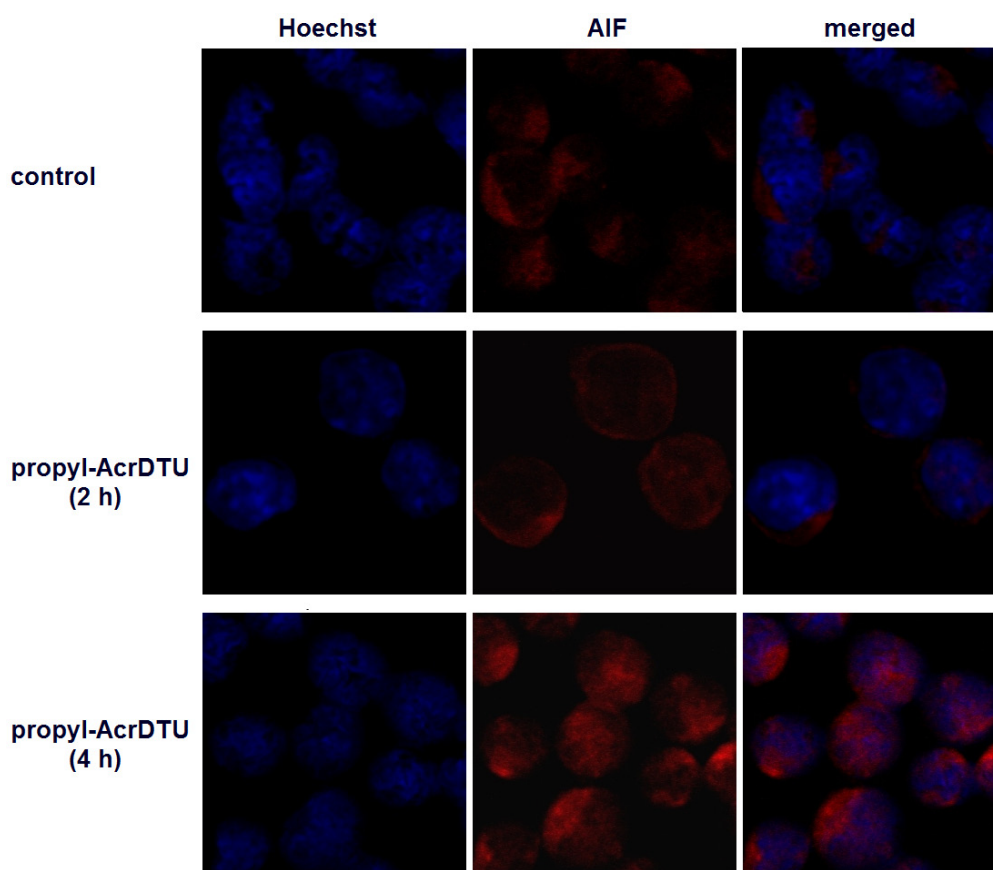


Figure 5. Mitochondrio-nuclear AIF translocation after PDT/propyl-AcrDTU. Cells were left untreated (control) or treated with 1 μ M propyl-AcrDTU for 1 h and irradiated (365 nm, 1.05 J/cm²). Cells were then cultured for 2 and 4 h, fixed with methanol, and stained with an antibody specific for AIF, followed by labeling with the secondary antibody (IgG TexasRed, red fluorescence). The nuclei were stained with Hoechst 33342 (blue fluorescence). Nuclear translocation of AIF is manifested by the overlap of AIF and nuclear staining in blue-violet. Representative examples of cells displaying translocation of AIF into the nucleus in treated cells (confocal microscopy, 63 \times /1.4 oil objective) are shown.

Table 3. Comparison of cathepsin B and D gene expression* in L1210/S and L1210/VCR cells.

	cathepsin B	cathepsin D
L12310/S	1	1
L1210/VCR	0.007089	0.115244

Note: *Expression of cathepsins was compared by the Livak method (see Materials and methods).

AcrDTU was not detected in the nuclei of non-irradiated cells (Figure 4). Only after irradiation, it was partly found in the nuclei of L1210/VCR cells (Figure 4).

Discussion

Despite the success of PDT against cancer cells, new compounds are still under investigation to improve the use of PDT in clinical oncology. The photo-inducible properties of acridine orange have been known for decades and it is not surprising that PDT using acridine orange to treat synovial

sarcoma, malignant musculoskeletal tumors, and even mouse osteosarcoma MDR [30–35] stimulated the preparation of new acridine derivatives as potential photosensitizers [21–28, 50]. We have recently reported that acridine derivatives, AcrDTUs, have photocytotoxic activity against mouse leukemia L1210 cells [36]. Our current research efforts have been directed to overcoming the resistance of mouse leukemia cells using the L1210/VCR cell subline as a chemo-resistant cell model. Cytotoxicity monitoring clearly showed that overexpression of P-gp (L1210/VCR) reduced the vincristine cytotoxicity by about 25-fold, while the cytotoxicity of AcrDTUs was only 1.5–2-fold, and the photocytotoxicity of AcrDTUs against resistant cells was 2–3-fold less than against L1210/S.

AcrDTU photocytotoxicity against L1210/VCR cells was slightly lower than against L1210/S cells. Recently, nestin expression was confirmed only in resistant L1210/VCR, but not in the sensitive cells [51]. Nestin (an intermediate filament protein) was involved as an organizer of signaling molecules and exhibited a distinct cytoprotective effect.

Nestin expression was related to the sensitivity of cells to oxidatively induced cell death [52]. Hypothetically, nestin could protect cells from cell death caused by oxidative stress.

L1210/VCR resistant cells were prepared by stepwise adaptation of the parental L1210 cell line to vincristine [37]. Unlike vincristine, propyl-AcrDTU was not effectively exported from the cells by a P-gp pump. Verapamil (a P-gp inhibitor) had only a modest effect on the photocytotoxicity of propyl-AcrDTUs. Vincristine induces not only overexpression of P-gp but also remodeling of cell surface saccharides. The sensitive cells were shown to have a more negative cell surface (probably higher sialic acid content) than the resistant L1210/VCR cells [53]. Although AcrDTUs may exist in a protonated form, we conclude that differences in cell surfaces between sensitive and resistant cells have no significant effect on the cellular uptake of these acridines. Although the accumulation of propyl-AcrDTU was similar in sensitive and resistant cells, the intracellular localization of AcrDTU was different. PSs for oncological PDTs sequester mainly in lysosomes or mitochondria [15, 33, 54–58] and it has been confirmed that PDT/AO targets lysosomes in cancer cells [29, 34]. Our previous studies have shown that propyl-AcrDTU was sequestered mainly in the lysosomes of L1210/S cells and partially in mitochondria [36], PDT/AcrDTU of the sensitive cells resulted in caspase-independent cell death, and release of cathepsins into the cytosol (due to damage of the lysosomal membrane after ROS formation) was crucial for the initiation of cell death. MDR may be associated with the lysosomal sequestration of chemotherapeutic agents. Zhitomirsky and Assaraf [58] showed that the number of drug-storing lysosomes per cell correlated directly with the extent of cellular resistance to these drugs. However, unlike the sensitive cell line L1210, sequestration of propyl-AcrDTU in the lysosomes of resistant L1210/VCR cells was not confirmed by flow cytometry. Since lysosomal cathepsins play an important role in cell death following PDT/propyl-AcrDTU in L1210/S [36], the expression of cathepsins (B and D) in the sensitive and resistant cells was evaluated. Surprisingly, RT-PCR analysis showed that the cathepsin mRNAs level in L1210/VCR cells was very low compared to that in sensitive L1210 cells. We conclude that, unlike sensitive cells, lysosomes are not a target organelle in resistant cells.

As mentioned above, the mitochondrion is considered to be a target for anticancer drugs including photosensitizers [59]. Our study of intracellular distribution of propyl-AcrDTUs confirmed the localization of this drug in mitochondria of sensitive L1210 cells and resistant cells. After irradiation, the overload of MitoRed with propyl-AcrDTU reached almost 62% of resistant cells. As expected, ROS generation led to mitochondrial membrane damage and ATP levels showed a rapid decrease: ATP levels decreased by about 60% in resistant cells (6 h after PDT). Necrosis was expected after the PDT, but surprisingly a decrease in ATP levels was not associated with the release of LDH from cells. Morphological changes in treated cells (cell shrinkage) and the formation of

a “DNA ladder” suggest that PDT can induce apoptotic cell death. But, activation of caspases was not observed (results not shown). We hypothesized that the observed intranucleosomal DNA fragmentation could be stimulated by the mitochondrial AIF protein (apoptosis inducing factor). AIF is a caspase-independent death effector and oxidative damage can induce nuclear translocation of AIF, which may represent an alternative route of death in absence of caspase activity [60]. The mitochondrio-nuclear translocation of AIF after PDT/propyl-AcrDTU was indeed confirmed by confocal microscopy. We suppose that a lower concentration of propyl-AcrDTU ($\leq 1 \mu\text{M}$) can inhibit metabolic activity and cell proliferation, and other signs of cell death will be detectable only after application of a higher concentration of AcrDTU or prolonged cell treatment (>24 h).

Although acridine derivatives are known as mutagens [61–62], not all of them can enter the nuclei [28, 63–66]. Propyl-AcrDTU was not located in the nuclei of L1210/VCR cells, although partial relocation of AcrDTU to the nuclei was observed after irradiation of the treated cells.

In summary, AcrDTUs is a family of photosensitizers also suitable for PDT of resistant L1210/VCR cells. The mechanism of cell death induced by AcrDTU is associated with its intracellular distribution and there is clear evidence that nuclei are not the target of these photosensitizers. Localization of propyl-AcrDTU in mitochondria, ATP depletion, mitochondrio-nuclear translocation of AIF followed by cell shrinkage, and intranucleosomal DNA fragmentation suggest that mitochondria play an important role in the cell death induced by PDT with propyl-AcrDTU. PDT/AcrDTU can lead to several types of cell death (necrosis or caspase-independent apoptosis).

Acknowledgments: Financial support for this work from the EU Structural Funds (ITMS: 26240220071) and the VEGA Grant Agency of the Ministry of Education of the Slovak Republic (1/0016/18, 1/0136/18, 2/0052/18) and APVV 14-0334 is gratefully acknowledged.

References

- [1] MARIN JJG, BRIZ O, RODRÍGUEZ-MACIAS G, DíEZ-MARTÍN JL, MACIAS RIR. Role of drug transport and metabolism in the chemoresistance of acute myeloid leukemia. *Blood Rev* 2016; 30: 55–64. <https://doi.org/10.1016/j.blre.2015.08.001>
- [2] CHEN Z, SHI T, ZHANG L, ZHU P, DENG M et al. Mammalian drug efflux transporters of the ATP binding cassette (ABC) family in multidrug resistance: A review of the past decade. *Cancer Lett* 2016; 370: 153–164. <https://doi.org/10.1016/j.canlet.2015.10.010>
- [3] JOYCE H, MCCANN A, CLYNES M, LARKIN A. Influence of multidrug resistance and drug transport proteins on chemotherapy drug metabolism. *Expert Opin Drug Metab Toxicol* 2015; 1: 795–809. <https://doi.org/10.1517/17425255.2015.1028356>

- [4] LIU Y, LI Q, ZHOU L, XIE N, NICE EC et al. Cancer drug resistance: redox resetting renders a way. *Oncotarget* 2016; 7: 42740–42761. <https://doi.org/10.18632/oncotarget.8600>
- [5] KACHALAKI S, EBRAHIMI M, KHOSROSHAHI LM, MOHAMMADINEJAD S, BARADARAN B. Cancer chemoresistance; biochemical and molecular aspects: a brief overview. *Eur J Pharm Sci* 2016; 89: 20–30. <https://doi.org/10.1016/j.ejps.2016.03.025>
- [6] WEYERGANG A, BERSTAD ME, BULL-HANSEN B, OLSEN CE, SELBO PK et al. Photochemical activation of drugs for the treatment of therapy-resistant cancers. *Photochem Photobiol Sci* 2015; 14: 1465–1475. <https://doi.org/10.1039/c5pp00029g>
- [7] CHEN JJ, LIU SP, ZHAO J, WANG SC, LIU TJ et al. Effects of a novel photoactivated photosensitizer on MDR1 over-expressing human breast cancer cells. *J Photochem Photobiol B* 2017; 171: 67–74. <https://doi.org/10.1016/j.jphotobiol.2017.04.037>
- [8] SPRING BQ, RIZVI I, XU N, HASAN T. The role of photodynamic therapy in overcoming cancer drug resistance. *Photochem Photobiol Sci* 2015; 14: 1476–1491. <https://doi.org/10.1039/c4pp00495g>
- [9] HUANG Z, HSU YC, LI LB, WANG LW, SONG XD et al. Photodynamic therapy of cancer – Challenges of multidrug resistance. *J Innov Opt Health Sci* 2015; 8: 1–13. <https://doi.org/10.1142/S1793545815300025>
- [10] BYVALTSEV VA, BARDONOVA LA, ONAKA NR, PPLKIN RA, OCHKAL SV et al. Acridine Orange: A Review of Novel Applications for Surgical Cancer Imaging and Therapy. *Front Oncol* 2019; 9: 925. <https://doi.org/10.3389/fonc.2019.00925>
- [11] BUGDE P, BISWAS R, MERIEN F, LU J, LIU DX et al. The therapeutic potential of targeting ABC transporters to combat multi-drug resistance. *Expert Opin Ther Targets* 2017; 21: 511–530. <https://doi.org/10.1080/14728222.2017.1310841>
- [12] BREIER A, GIBALOVA L, SERES M, BARANCIK M, SULOVA Z. New insight into p-glycoprotein as a drug target. *Anticancer Agents Med Chem* 2013; 13: 159–170.
- [13] POKHAREL D, ROSEBLADE A, OENARTO V, LU JF, BEBAWY M. Proteins regulating the intercellular transfer and function of P-glycoprotein in multidrug-resistant cancer. *Ecancermedalscience* 2017; 11: 768. <https://doi.org/10.3332/ecancer.2017.768>
- [14] JENDZELOVSKY R, MIKES J, KOVAL J, SOUCEK K, PROCHAZKOVA J et al. Drug efflux transporters, MRP1 and BCRP, affect the outcome of hypericin-mediated photodynamic therapy in HT-29 adenocarcinoma cells. *Photochem Photobiol Sci*. 2009; 8: 1716–1723. <https://doi.org/10.1039/b9pp00086k>
- [15] KUSUZAKI K, MINAMI G, TAKESHITA H, MURATA H, HASHIGUCHI S et al. Photodynamic inactivation with acridine orange on a multidrug-resistant mouse osteosarcoma cell line. *Jpn J Cancer Res* 2000; 91: 439–445. <https://doi.org/10.1111/j.1349-7006.2000.tb00964.x>
- [16] TRINDADE GS, FARIAS SL, RUMJANEK VM, CAPELLA MA. Methylene blue reverts multidrug resistance: sensitivity of multidrug resistant cells to this dye and its photodynamic action. *Cancer Lett* 2000; 151: 161–167. [https://doi.org/10.1016/s0304-3835\(99\)00408-5](https://doi.org/10.1016/s0304-3835(99)00408-5)
- [17] DIEZ B, ERNST G, TEIJO MJ, BATTLE A, HAJOS S et al. Combined chemotherapy and ALA-based photodynamic therapy in leukemic murine cells. *Leuk Res* 2012; 36: 1179–1184. <https://doi.org/10.1016/j.leukres.2012.04.027>
- [18] TANG PM, ZHANG DM, XUAN NH, TSUI SK, WAYE MM et al. Photodynamic therapy inhibits P-glycoprotein mediated multidrug resistance via JNK activation in human hepatocellular carcinoma using the photosensitizer pheophorbide a. *Mol Cancer*. 2009; 8: 56. <https://doi.org/10.1186/1476-4598-8-56>
- [19] KOŽURKOVÁ M, SABOLOVÁ D, KRISTIAN P. A review on acridinylthioureas and its derivatives: biological and cytotoxic activity. *J Appl Toxicol* 2017; 37: 1132–1139. <https://doi.org/10.1002/jat.3464>
- [20] GENSICKA-KOWALEWSKA M, CHOLEWIŃSKI G, DZIERZBICKA K. Recent developments in the synthesis and biological activity of acridine/acridone analogues. *RSC Adv* 2017; 7: 15776–15804. <https://doi.org/10.1039/C7RA01026E>
- [21] DICHARA M, PREZZAVENTO O, MARRAZZO A, PITTALÀ V, SALERNO L et al. Recent advances in drug discovery of phototherapeutic non-porphyrinic anticancer agents. *Eur J Med Chem*. 2017; 142: 459–485. <https://doi.org/10.1016/j.ejmech.2017.08.070>
- [22] FU W, LI X, LU X, ZHANG L, LI R et al. A novel acridine derivative, LS-1-10 inhibits autophagic degradation and triggers apoptosis in colon cancer cells. *Cell Death Dis* 2017; 8: e3086. <https://doi.org/10.1038/cddis.2017.498>
- [23] LANG X, LI L, CHEN Y, SUN Q, WU Q et al. Novel synthetic acridine derivatives as potent DNA-binding and apoptosis-inducing antitumor agents. *Bioorg Med Chem* 2013; 21: 4170–4177. <https://doi.org/10.1016/j.bmc.2013.05.008>
- [24] SCHMIDT A, LIU M. Recent Advances in the Chemistry of Acridines. *Advances in Heterocyclic Chemistry* 2015; 115: 287–353. <https://doi.org/10.1016/BS.AIHCH.2015.04.004>
- [25] DI GIORGIO C, NIKOYAN A, DECOME L, BOTTA C, ROBIN M et al. DNA-damaging activity and mutagenicity of 16 newly synthesized thiazolo[5,4-a]acridine derivatives with high photo-inducible cytotoxicity. *Mutat Res* 2008; 650: 104–114. <https://doi.org/10.1016/j.mrgentox.2007.10.022>
- [26] BENCHABANE Y, DI GIORGIO C, BOYER G, SABATIER AS, ALLEGRO D et al. Photo-inducible cytotoxic and clastogenic activities of 3,6-disubstituted acridines obtained by acylation of proflavine. *Eur J Med Chem* 2009; 44: 2459–2467. <https://doi.org/10.1016/j.ejmech.2009.01.010>
- [27] GRANT KB, TERRY CA, GUDE L, FERNÁNDEZ MJ, LORENTE A. Synthesis and DNA photocleavage by a pyridine-linked bis-acridine chromophore in the presence of copper(II): ionic strength effects. *Bioorg Med Chem Lett* 2011; 21: 1047–1051. <https://doi.org/10.1016/j.bmcl.2010.12.009>
- [28] ČIŽEKOVÁ L, GROLMUSOVÁ A, IPÓTHOVÁ Z, BARBIERIKOVÁ Z, BREZOVÁ V et al. Novel 3,6-bis(imidazolidine)acridines as effective photosensitizers for photodynamic therapy. *Bioorg Med Chem* 2014; 22: 4684–4693. <https://doi.org/10.1016/j.bmc.2014.07.013>

- [29] ZDOLSEK JM, OLSSON GM, BRUNK UT. Photooxidative damage to lysosomes of cultured macrophages by acridine orange. *Photochem Photobiol* 1990; 51: 67–76. <https://doi.org/10.1111/j.1751-1097.1990.tb01685.x>
- [30] FOTIA C, AVNET S, KUSUZAKI K, RONCUZZI L, BALDINI N. Acridine Orange is an Effective Anti-Cancer Drug that Affects Mitochondrial Function in Osteosarcoma Cells. *Curr Pharm Des* 2015; 21: 4088–4094. <https://doi.org/10.2174/1381612821666150918144953>
- [31] KUSUZAKI K, AOMORI K, SUGINOSHITA T, MINAMI G, TAKESHITA H et al. Total tumor cell elimination with minimum damage to normal tissues in musculoskeletal sarcomas following photodynamic therapy with acridine orange. *Oncology* 2000; 59: 174–180. <https://doi.org/10.1159/000012156>
- [32] YOSHIDA K, KUSUZAKI K, MATSUBARA T, MATSUMINE A, KUMAMOTO T et al. Periosteal Ewing's sarcoma treated by photodynamic therapy with acridine orange. *Oncol Rep* 2005; 13: 279–282.
- [33] MATSUBARA T, KUSUZAKI K, MATSUMINE A, SHINTANI K, SATONAKA H et al. Acridine orange used for photodynamic therapy accumulates in malignant musculoskeletal tumors depending on pH gradient. *Anticancer Res* 2006; 26: 187–193.
- [34] KUSUZAKI K, MURATA H, MATSUBARA T, SATONAKA H, WAKABAYASHI T et al. Review. Acridine orange could be an innovative anticancer agent under photon energy. *In Vivo* 2007; 21: 205–214.
- [35] SATONAKA H, KUSUZAKI K, AKEDA K, TSUJII M, IINO T et al. Acridine orange inhibits pulmonary metastasis of mouse osteosarcoma. *Anticancer Res* 2011; 31: 4163–4168.
- [36] CISÁRIKOVÁ A, BARBIERIKOVÁ Z, JANOVEC L, IMRICH J, HUNÁKOVÁ L et al. Acridin-3,6-dialkyldithiurea hydrochlorides as new photosensitizers for photodynamic therapy of mouse leukemia cells. *Bioorg Med Chem* 2016; 24: 2011–2022. <https://doi.org/10.1016/j.bmc.2016.03.029>
- [37] POLEKOVÁ L, BARANČÍK M, MRÁZOVÁ T, PIRKER R, WALLNER J et al. Adaptation of mouse leukemia cells L1210 to vincristine. Evidence for expression of P-glycoprotein. *Neoplasma* 1992; 39: 73–77.
- [38] FIALA R, SULOVA Z, EL-SAGGAN AH, UHRÍK B, LIPTAJ T et al. P-glycoprotein-mediated multidrug resistance phenotype of L1210/VCR cells is associated with decreases of oligo- and/or polysaccharide contents. *Biochim Biophys Acta* 2003; 1639: 213–224. <https://doi.org/10.1016/j.bbadis.2003.09.009>
- [39] SULOVA Z, DITTE P, KURUCOVÁ T, POLÁKOVÁ E, ROGOZANOVÁ K et al. The presence of P-glycoprotein in L1210 cells directly induces down-regulation of cell surface saccharide targets of concanavalin A. *Anticancer Res* 2010; 30: 3661–3668.
- [40] VANTOVÁ Z, PAULÍKOVÁ H, SABOLOVÁ D, KOŽURKOVÁ M, SUCHÁNOVÁ M et al. Cytotoxic activity of acridin-3,6-diyl dithiurea hydrochlorides in human leukemia line HL-60 and resistant subline HL-60/ADR. *Int J Biol Macromol* 2009; 45: 174–180. <https://doi.org/10.1016/j.ijbiomac.2009.04.018>
- [41] CARMICHAEL J, DE GRAFF WG, GAZDAR AF, MINNA JD, MITCHELL JB. Evaluation of a tetrazolium-based semi-automated colorimetric assay: assessment of chemosensitivity testing. *Cancer Res* 1987; 47: 936–942.
- [42] GRIVELL AR, BERRY MN. The effects of phosphate- and substrate-free incubation conditions on glycolysis in Ehrlich ascites tumour cells. *Biochim Biophys Acta* 1996; 1291: 83–88. [https://doi.org/10.1016/0304-4165\(96\)00049-9](https://doi.org/10.1016/0304-4165(96)00049-9)
- [43] LIVAK KJ, SCHMITTGEN TD. Analysis of relative gene expression data using real-time quantitative PCR and the 2⁻(Delta Delta C(T)) Method. *Methods* 2001; 25: 402–408. <https://doi.org/10.1006/meth.2001.1262>
- [44] BOHÁČOVÁ V, KVAČKAJOVÁ J, BARANČÍK M, DROBNÁ Z, BREIER A. Glutathione S-transferase does not play a role in multidrug resistance of L1210/VCR cell line. *Physiol Res* 2000; 49: 447–453.
- [45] AHMAD N, FEYES DK, AGARWAL R, MUKHTAR H. Photodynamic therapy results in induction of WAF1/CIP1/P21 leading to cell cycle arrest and apoptosis. *Proc Natl Acad Sci USA* 1998; 95: 6977–6982. <https://doi.org/10.1073/pnas.95.12.6977>
- [46] VANTIEGHEM A, XU Y, ASSEFA Z, PIETTE J, VANDENHEEDE JR et al. Phosphorylation of Bcl-2 in G2/M phase-arrested cells following photodynamic therapy with hypericin involves a CDK1-mediated signal and delays the onset of apoptosis. *Biol Chem* 2002; 277: 37718–37731. <https://doi.org/10.1074/jbc.M204348200>
- [47] SASNAUSKIENE A, KADZIAUSKAS J, VEZELYTE N, JONUSIENE V, KIRVELIENE V. Apoptosis, autophagy and cell cycle arrest following photodamage to mitochondrial interior. *Apoptosis* 2009; 14: 276–286. <https://doi.org/10.1007/s10495-008-0292-8>
- [48] LIU J, ZHENG L, LI Y, ZHANG Z, ZHANG L et al. Effect of DTPP-mediated photodynamic therapy on cell morphology, viability, cell cycle, and cytotoxicity in a murine lung adenocarcinoma cell line. *Lasers Med Sci* 2015; 30: 181–191. <https://doi.org/10.1007/s10103-014-1637-x>
- [49] BARANČÍK M, POLEKOVÁ L, MRÁZOVÁ T, BREIER A, STANKOVIČOVÁ T et al. Reversal effects of several Ca(2+)-entry blockers, neuroleptics and local anaesthetics on P-glycoprotein-mediated vincristine resistance of L1210/VCR mouse leukaemic cell line. *Drugs Exp Clin Res* 1994; 20: 13–18.
- [50] ADAR Y, STARK M, BRAM EE, NOWAK-SLIWINSKA P, VAN DEN BERGH H et al. Imidazoacridinone-dependent lysosomal photodestruction: a pharmacological Trojan horse approach to eradicate multidrug-resistant cancers. *Cell Death Dis* 2012; 3: e293. <https://doi.org/10.1038/cddis.2012.30>
- [51] COCULOVÁ M, IMRICHOVÁ D, ŠEREŠ M, MESSINGEROVÁ L, BOHÁČOVÁ V et al. The expression of P-glycoprotein in leukemia cells is associated with the upregulated expression of nestin, a class 6 filament protein. *Leuk Res* 48: 32–39. <https://doi.org/10.1016/j.leukres.2016.05.021>
- [52] SAHLGREN CM, PALLARI HM, HE T, CHOU YH, GOLDMAN RD et al. A nestin scaffold links Cdk5/p35 signaling to oxidant-induced cell death. *Embo J* 2006; 25: 4808–4819. <https://doi.org/10.1038/sj.emboj.7601366>

- [53] SULOVÁ Z, MISLOVICOVÁ D, GIBALOVÁ L, VAJCNEROVÁ Z, POLÁKOVÁ E et al. Vincristine-induced overexpression of P-glycoprotein in l1210 cells is associated with remodeling of cell surface saccharides. *J Proteome Res* 2009; 8: 513–520. <https://doi.org/10.1021/pr8007094>
- [54] GÈZE M, MORLIÈRE P, MAZIÈRE JC, SMITH KM, SANTUS R. Lysosomes, a key target of hydrophobic photosensitizers proposed for photochemotherapeutic applications. *J Photochem Photobiol B* 1993; 20: 23–35. [https://doi.org/10.1016/1011-1344\(93\)80128-v](https://doi.org/10.1016/1011-1344(93)80128-v)
- [55] PENG TI, CHANG CJ, GUO MJ, WANG YH, YU JS et al. Mitochondrion-targeted photosensitizer enhances the photodynamic effect-induced mitochondrial dysfunction and apoptosis. *Ann N Y Acad Sci* 2005; 1042: 419–428. <https://doi.org/10.1196/annals.1338.035>
- [56] MARINO J, GARCÍA VIOR MC, FURMENTO VA, BLANK VC, AWRUCH J et al. Lysosomal and mitochondrial permeabilization mediates zinc(II) cationic phthalocyanine phototoxicity. *Int J Biochem Cell Biol* 2013; 45: 2553–2562. <https://doi.org/10.1016/j.biocel.2013.08.012>
- [57] RAJAPUTRA P, NKEPANG G, WATLEY R, YOU Y. Synthesis and in vitro biological evaluation of lipophilic cation conjugated photosensitizers for targeting mitochondria. *Bioorg Med Chem* 2013; 21: 379–387. <https://doi.org/10.1016/j.bmc.2012.11.032>
- [58] ZHITOMIRSKY B, ASSARAF YG. Lysosomes as mediators of drug resistance in cancer. *Drug Resist Updat* 2016; 24: 23–33. <https://doi.org/10.1016/j.drug.2015.11.004>
- [59] SZEWCZYK A, WOJTCZAK L. Mitochondria as a pharmacological target. *Pharmacol Rev* 2002; 54: 101–127. <https://doi.org/10.1124/pr.54.1.101>
- [60] CREGAN SP, DAWSON VL, SLACK RS. Role of AIF in caspase-dependent and caspase-independent cell death. *Oncogene* 2004; 23: 2785–2796. <https://doi.org/10.1038/sj.onc.1207517>
- [61] KALINOWSKA E, CHORAZY M. Mutagenic activity of some 9-aminoalkyl acridine derivatives on *S. typhimurium*. *Mutat Res* 1980; 78: 7–15. [https://doi.org/10.1016/0165-1218\(80\)90020-8](https://doi.org/10.1016/0165-1218(80)90020-8)
- [62] FERGUSON LR, DENNY WA. The genetic toxicology of acridines. *Mutat Res* 1991; 258: 123–160. [https://doi.org/10.1016/0165-1110\(91\)90006-h](https://doi.org/10.1016/0165-1110(91)90006-h)
- [63] DICKENS BF, WEGGLICKI WB, BOEHME PA, MAK TI. Antioxidant and lysosomotropic properties of acridine-propranolol: protection against oxidative endothelial cell injury. *J Mol Cell Cardiol* 2002; 34: 129–137. <https://doi.org/10.1006/jmcc.2001.1495>
- [64] PEIXOTO P, ZEGHIDA W, CARREZ D, WU TD, WATTEZ N et al. Unusual cellular uptake of cytotoxic 4-hydroxymethyl-3-aminoacridine. *Eur J Med Chem* 2009; 44: 4758–463. <https://doi.org/10.1016/j.ejmech.2009.06.034>
- [65] KRAJŇÁKOVÁ L, PAULÍKOVÁ H, BAČOVÁ Z, BAKOŠ J, JANOVEC L et al. Intracellular distribution of 3,6-bis(3-alkylguanidino)acridines determines their cytotoxicity. *Neoplasma* 2015; 62: 98–107. https://doi.org/10.4149/neo_2015_012
- [66] IPÓTHOVÁ Z, PAULÍKOVÁ H, ČIŽEKOVÁ L, HUNÁKOVÁ L, LABUDO VÁ M et al. Subcellular localization of proflavine derivative and induction of oxidative stress – in vitro studies. *Bioorg Med Chem* 2013; 21: 6726–6731. <https://doi.org/10.1016/j.bmc.2013.08.007>